Supplementary Information

The first homochiral coordination polymer with temperature-independent piezoelectric and dielectric properties

Peng Yang,[a] Xiang He,[a] Ming-Xing Li,*[,a] Qiong Ye,[b] Jia-Zhen Ge,[b] Zhao-Xi Wang,[a] Shou-Rong Zhu,[a] Min Shao,[c] and Hong-Ling Cai*[,b]

[a] Department of Chemistry, College of Sciences, Shanghai University, Shanghai 200444, China.

[b] Ordered Matter Science Research Center, Southeast University, Nanjing, 211189, China.

[c] Laboratory for Microstructures, Shanghai University, Shanghai 200444, China

* Corresponding authors: E-mail: mx_li@mail.shu.edu.cn; hlcai@seu.edu.cn.

Physical Measurements： Elemental analyses for C, H and N were carried out with a Vario EL III elemental analyzer. Infrared spectra were recorded with a Nicolet A370 FT-IR spectrometer using KBr pellets in the 4000–400 cm^{-1} region. Powder X-ray diffraction (PXRD) data were recorded on a Rigaku DLMAX-2550 diffractometer. Thermal analyses were completed on a Mettler Toledo TGA/SDTA85e thermal analyzer at a heating rate of 10 °C min^{-1} in N_2 atmosphere. Circular dichroism (CD) spectrum measurements were performed using a JASCO J-810 spectropolarimeter. The temperature dependence of the piezoelectric coefficient of d22 was measured using a PM200 piezometer system. The permittivity measurements of pressed powder slices with dimensions of 3×3 mm^2 were performed using an automatic impedance HP4191A analyzer with frequency of 100 to 1M Hz. The samples were pretreated by heating to 170°C to remove the moisture and lattice water.

X-ray crystallography: Suitable single crystals of complexes **1** and **2** were selected for X-ray diffraction study. Data collections were performed with graphite-monochromatic Mo $K\alpha$ radiation (λ = 0.71073 Å) on a Bruker Smart Apex-II CCD diffractometer at T = 293(2) K. Determinations of the crystal system, orientation

matrix, and cell dimensions were performed according to the established procedures. Lorentz polarization and absorption correction were applied. The structures were solved by the direct method and refined by full-matrix least-squares on F^2 with SHELXTL-97 program. All non-hydrogen atoms were refined anisotropically, and hydrogen atoms were located and included at their calculated positions. The crystallographic data and structural refinement results are summarized in Table S1. The selected bond distances and angles are listed in Table S2.

Table S1. Crystallographic data and structural refinements for **1** and **2**

Complex	**1**	**2**
Formula	$C_{44}H_{52}N_8O_{12}Mn_2$	$C_{44}H_{64}N_{12}O_{16}Co_2$
Formula weight	994.82	1134.93
Crystal system	Monoclinic	Monoclinic
Space group	*C*2	$P2_1$
a (Å)	21.756(4)	7.521(12)
b (Å)	11.090(2)	17.21(3)
c (Å)	11.085(2)	19.15(3)
α (°)	90	90
β (°)	119.155(2)	95.26(2)
γ (°)	90	90
V (Å^3)	2335.7(8)	2468(7)
Z	2	2
D_c (g cm^{-3})	1.414	1.527
F(000)	1036	1188
μ (mm^{-1})	0.610	0.755
Reflections collected / unique	6076 / 3666	12048 / 8390
R_{int}	0.0184	0.0909
Data / restraints / parameters	3666 / 1 / 304	8390 / 3 / 674
GOF (F^2)	1.045	1.035
R_1, wR_2 ($I>2\sigma(I)$)[a]	0.0246, 0.0621	0.0738, 0.1243
R_1, wR_2 (all data)[b]	0.0264, 0.0632	0.1661, 0.1502
Flack parameter	0.016(13)	−0.01(2)
Largest diff. peak and hole (e Å^{-3})	0.310, −0.235	0.618, −0.863

[a] $R_1 = \sum||F_o|-|F_c||/\sum|F_o|$. [b] $wR_2 = [\sum w(F_o^2-F_c^2)^2/\sum w(F_o^2)^2]^{1/2}$.

Table S2. Selected bond distances (Å) and angles (°) for **1** and **2**

Complex **1**[a]			
Mn(1)-O(1)	2.090(2)	Mn(2)-O(3)	2.103(2)
Mn(1)-N(1)	2.293(2)	Mn(2)-N(3)	2.309(2)
Mn(1)-N(2)	2.359(2)	Mn(2)-N(4)	2.327(2)
N(1)-Mn(1)-N(1)#1	152.79(10)	N(3)-Mn(2)-N(3)#2	149.61(10)
O(1)-Mn(1)-N(2)#1	164.55 (7)	O(3)-Mn(2)-N(4)#2	167.06 (7)
O(1)#1-Mn(1)-N(2)	164.55 (7)	O(3)#2-Mn(2)-N(4)	167.06 (7)
N(2)#1-Mn(1)-N(2)	76.56(10)	O(3)-Mn(2)-N(3)	99.57(7)
N(1)-Mn(1)-N(2)#1	88.21(7)	O(3)#2-Mn(2)-N(3)	99.62(7)
O(1)-Mn(1)-N(1)	95.93(7)	O(3)-Mn(2)-N(4)	88.98(7)
O(1)-Mn(1)-N(2)	90.81(7)	O(3)-Mn(2)-O(3)#2	101.04(10)
O(1)-Mn(1)-O(1) #1	102.95(10)	N(3)-Mn(2)-N(4)#2	86.65(6)
O(1)-Mn(1)-N(1)#1	100.94(7)	N(3)-Mn(2)-N(4)	70.36(7)
Complex **2**[b]			
Co(1)-O(1)	2.043(7)	Co(2)-O(4)	1.945(7)
Co(1)-N(7)	2.166(9)	Co(2)-O(5)	2.033(8)
Co(1)-N(1)	2.220(8)	Co(2)-O(6)	2.193(8)
Co(1)-O(1W)	2.044(8)	Co(2)-N(12)#2	2.089(8)
Co(1)-O(2W)	2.063(8)	Co(2)-N(6)#1	2.069(9)
Co(1)-O(3W)	2.129(7)		
O(1)-Co(1)-O(3W)	177.0(3)	O(4)-Co(2)-O(6)	172.6(4)
N(7)-Co(1)-N(1)	168.8(3)	O(5)-Co(2)-N(6)#1	137.6(3)
O(1W)-Co(1)-O(2W)	177.3(3)	O(5)-Co(2)-N(12)	100.6(3)
O(1)-Co(1)-O(2W)	91.3(3)	N(6)#1-Co(2)-O(6)	88.9(3)
O(2W)-Co(1)-O(3W)	91.6(3)	N(6)#1-Co(2)-N(12)#2	108.0(4)
O(1)-Co(1)-N(1)	96.8(3)	O(4)-Co(2)-N(6)#1	97.9(3)
O(2W)-Co(1)-N(7)#1	92.0(3)	O(4)-Co(2)-O(5)	112.4(3)
O(1W)-Co(1)-N(1)	89.7(3)	O(4)-Co(2)-N(12)	91.1(3)
O(3W)-Co(1)-N(1)	83.9(3)	O(5)-Co(2)-O(6)	60.3(3)
O(1)-Co(1)-N(7)#1	94.4(3)	N(12)#2-Co(2)-O(6)	89.4(3)

Symmetry codes: [a] #1 -x+2, y, -z+2; #2 -x+1, y, -z+1. [b] #1 x+1, y, z+1; #2 x+1, y, z.

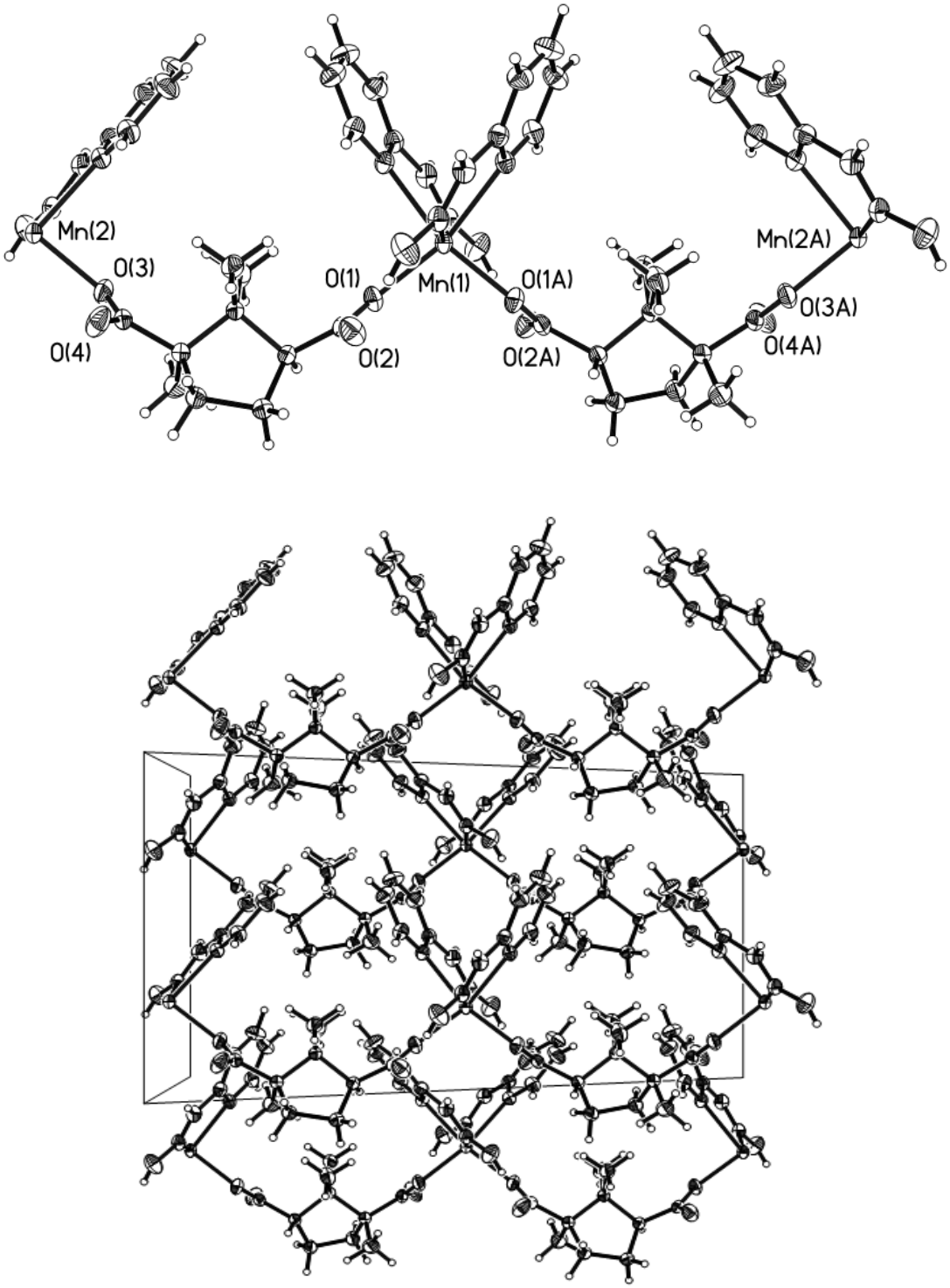

Fig. S1 The ORTEP diagram (top) and packing diagram (bottom) of complex **1**

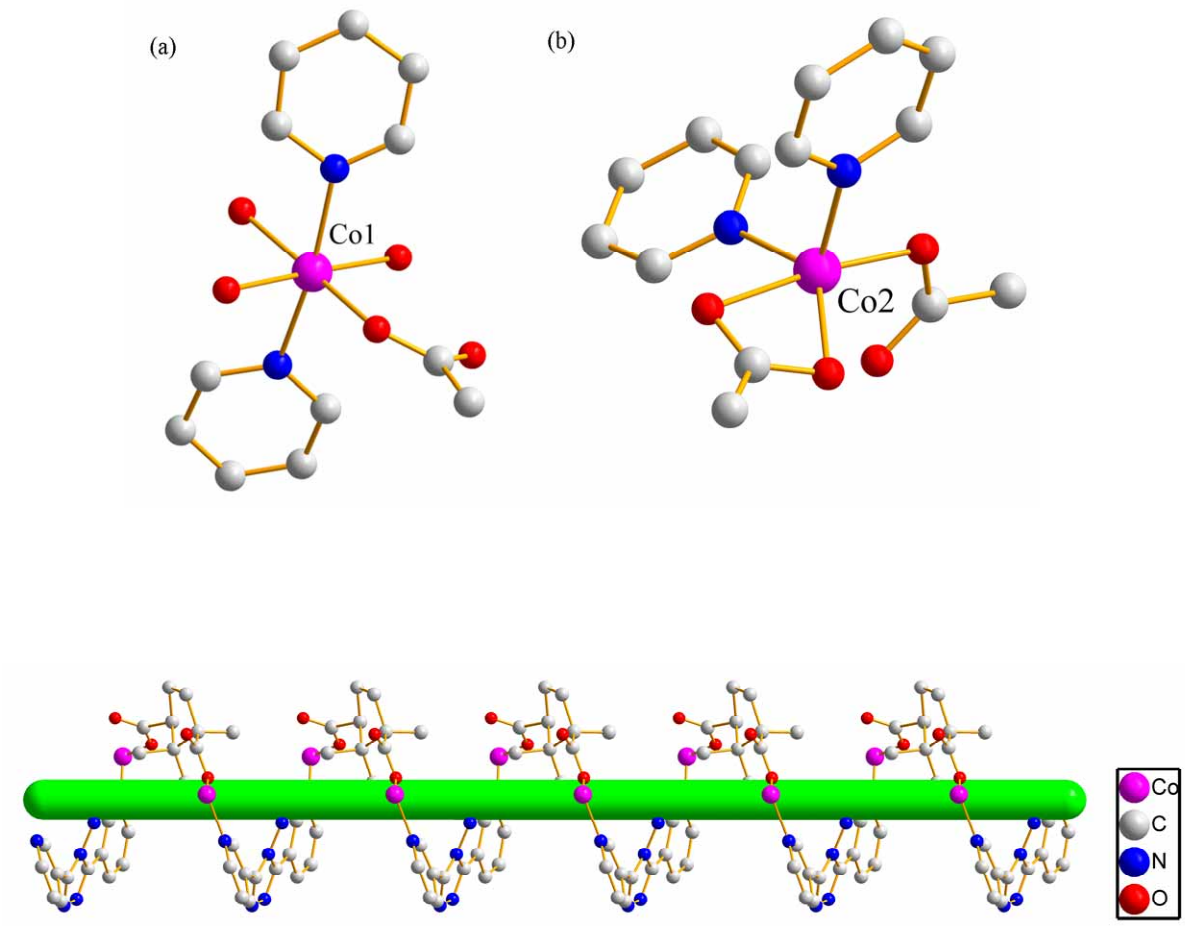

Fig. S2 Coordination environments around Co1 and Co2, and 1-D 3-abpt–Co–cam chain in complex **2**

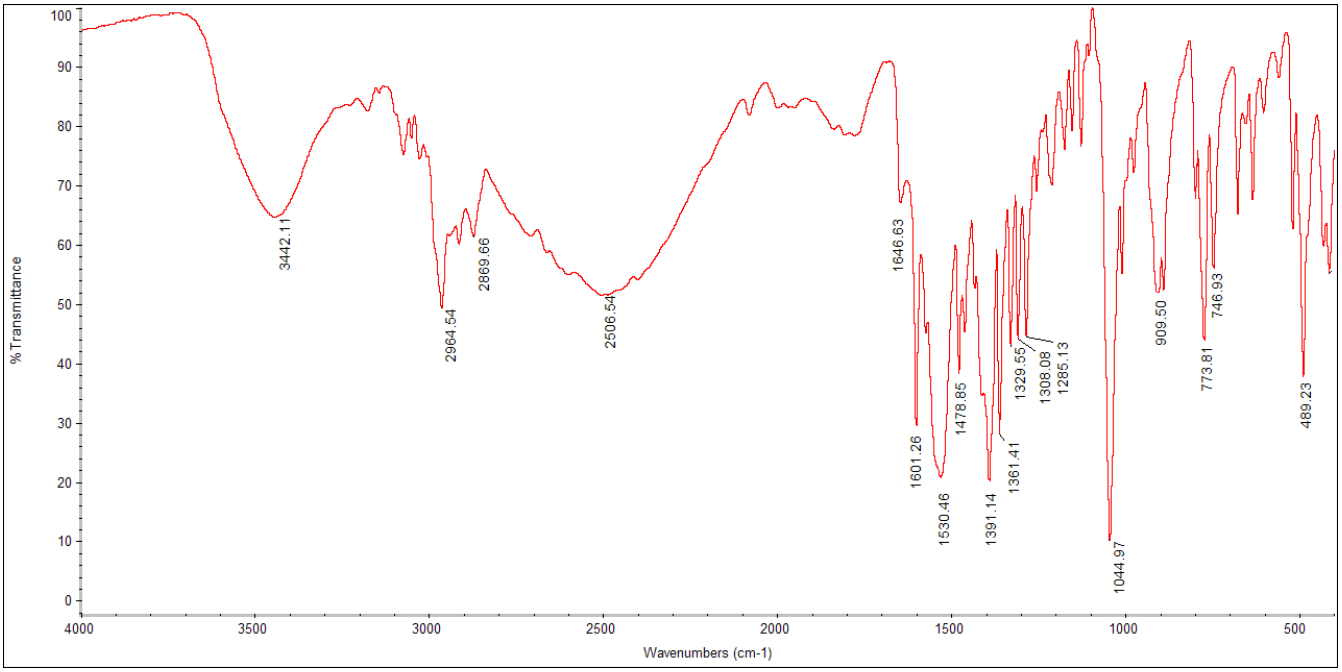

$[Mn_2(D\text{-cam})_2(2\text{-Hpao})_4]_n$ (**1**)

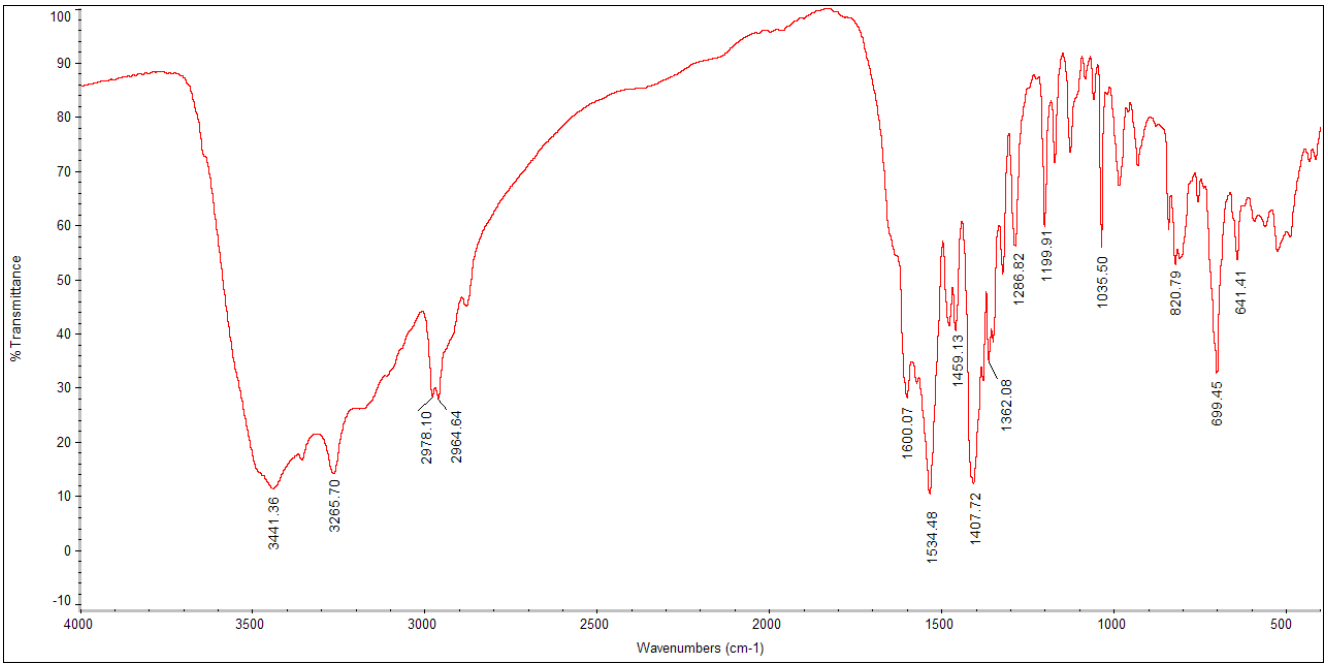

$[Co_2(D\text{-cam})_2(3\text{-abpt})_2(H_2O)_3]_n \cdot 5nH_2O$ (**2**)

Fig. S3 The IR spectra of complexes **1** and **2**

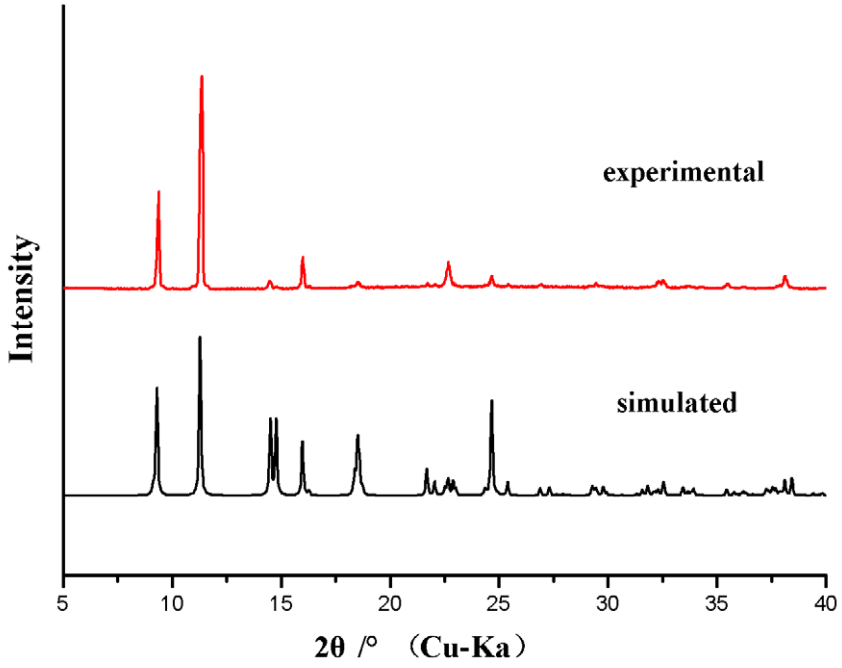

The PXRD pattern of **1**

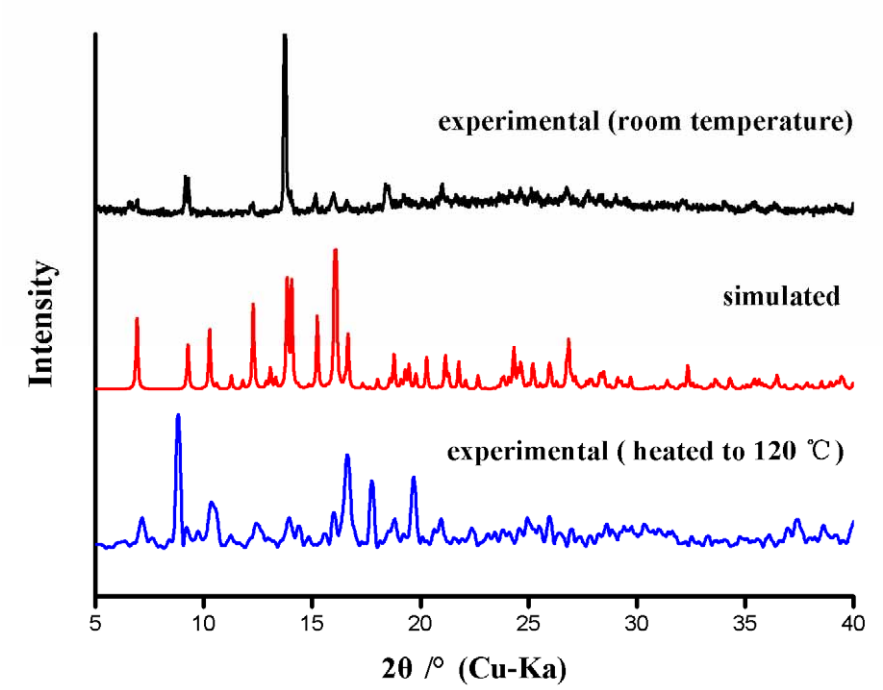

The PXRD pattern of **2**

TG-DSC showed complex **2** lost coordinated and lattice water in 50–115ºC. After heated **2** to 120ºC, PXRD showed the crystalline still maintained, but the structure may be a little change.

Fig. S4 The measured and simulated powder X-ray diffraction patterns of complexes **1** and **2**

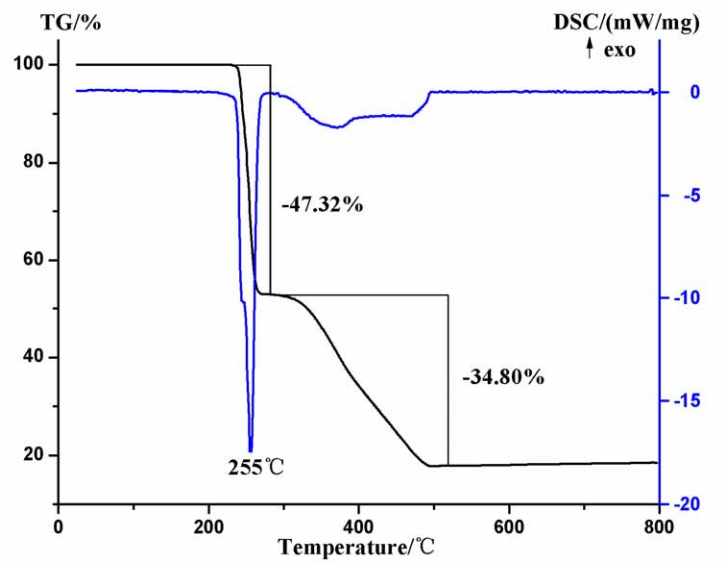

TG-DSC curves of **1**

Complex **1** remains stable until 230ºC and exhibits an explosive decomposition that is related to the loss of four 2-Hpao ligands in the range of 230–280ºC with an endothermic peak at 255ºC (found 47.32%, calcd 49.10%). The further weight-loss in the range of 320–500ºC indicates the decomposition of two D-cam ligands, leaving a final residue of MnO_2 (found 17.88%, calcd 17.48%).

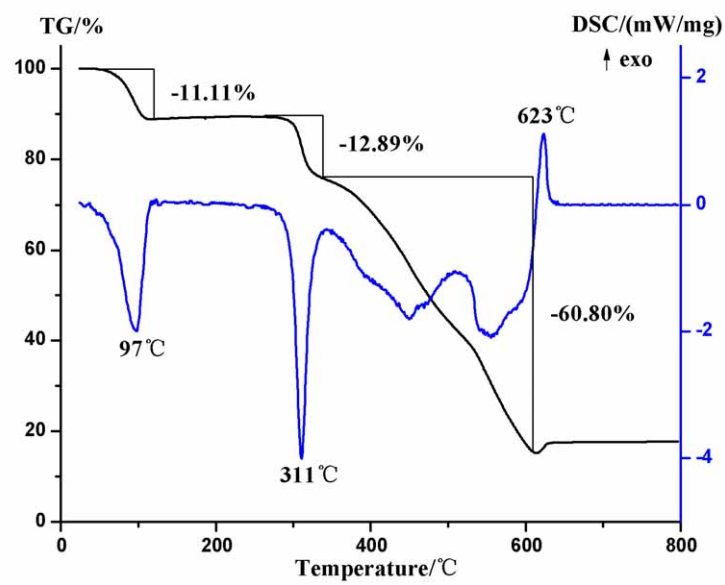

TG-DSC curves of **2**

Complex **2** displays a weight-loss of 11.11% in the range of 50–115ºC with an endothermic peak at 97ºC, corresponding to the expulsion of three coordinated water and five lattice water molecules (calcd 12.69%). The main framework remains stable until it is heated to 300ºC, and then loses 3-abpt and D-cam ligands gradually. The residue at 614ºC is CoO (found 15.20%, calcd 13.20%), which is further oxidized to Co_2O_3 accompanied by a strong exothermic peak at 623ºC.

Fig. S5 The thermal analysis curves of complexes **1** and **2**

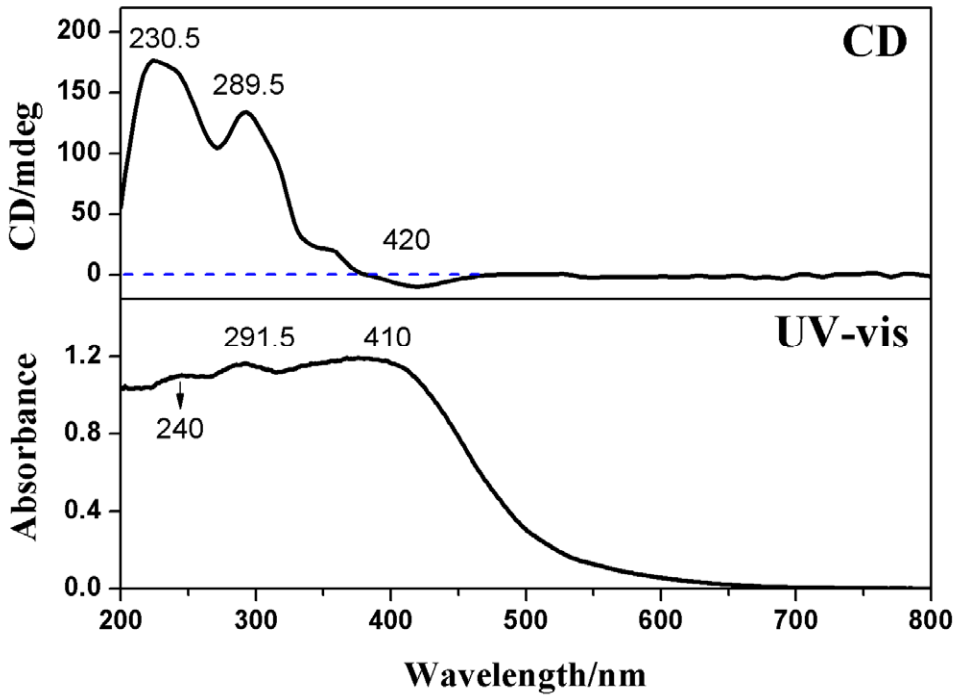

The CD and UV-vis spectra of **1**

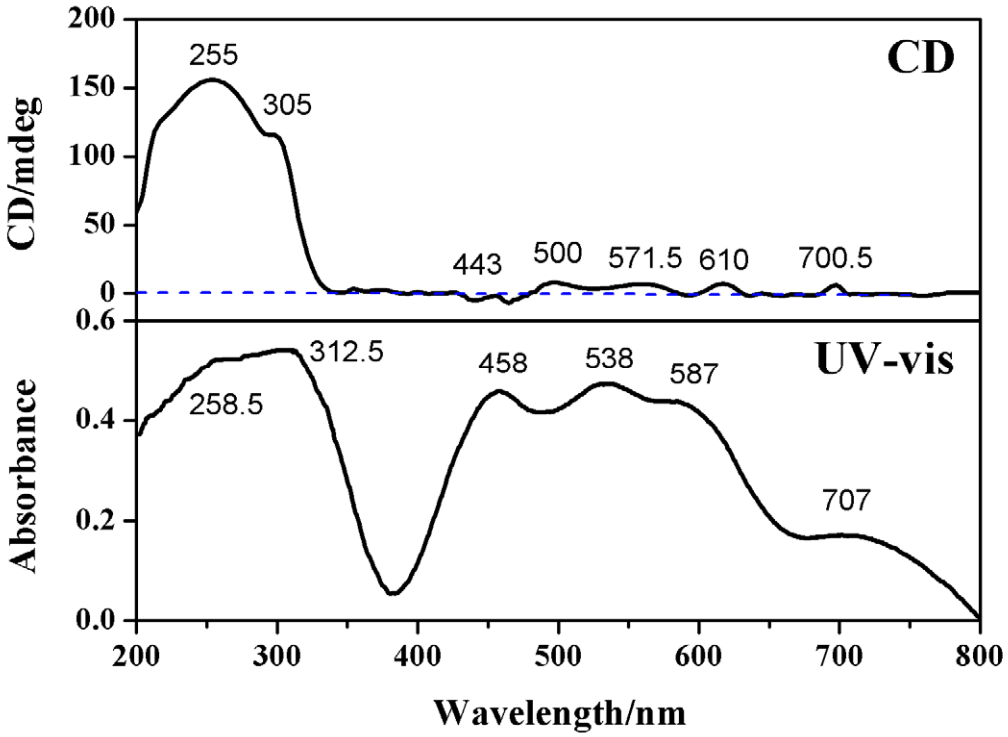

The CD and UV-vis spectra of **2**

Fig. S6 The solid state circular dichroism and UV-vis spectra of complexes **1** and **2**